# Hydration in the Various Phases of the Triblock Copolymers $EO_{13}PO_{30}EO_{13}$ (Pluronic L64) and $EO_6PO_{34}EO_6$ (Pluronic L62), Based on Electron Spin Resonance Spectra of Cationic Spin Probes

**Agneta Caragheorgheopol[†,‡] and Shulamith Schlick*[,‡]**

*Institute of Physical Chemistry "I.G. Murgulescu", Romanian Academy, Splaiul Independentei 202, 77208 Bucharest, Romania, and Department of Chemistry, University of Detroit Mercy, Detroit, Michigan 48219*

*Received June 23, 1998; Revised Manuscript Received September 9, 1998*

ABSTRACT: Aqueous solutions of the triblock copolymers poly(ethylene oxide)-*b*-poly(propylene oxide)-*b*-poly(ethylene oxide) $EO_{13}PO_{30}EO_{13}$ (Pluronic L64) and $EO_6PO_{34}EO_6$ (Pluronic L62) were investigated over a wide polymer concentration range (20−90% w/w) across all phases, from micellar to liquid crystalline and to reverse micellar phases. Electron spin resonance spectra of a homologous series of cationic nitroxide spin probes, CAT*n* (*n* is the number of carbon atoms in the alkyl substituent), were used to deduce the local polarity in the water-rich domains of the self-assembled polymer aggregates. The isotropic hyperfine splitting from the $^{14}N$ nucleus of the >NO fragment, $a_N$, was the polarity sensitive parameter; $a_N$ values were translated into *effective* local hydration values $Z_{eff}$ by reference to a series of PEO/water mixtures with water contents expressed as $Z = [H_2O]/[EO]$. By this approach it was possible to follow changes in the hydration of the EO blocks at various distances from the hydrophobic core in the L62 and L64 aggregates on a scale of ≤20 Å and to infer from these changes the mechanism of phase transitions. The results are consistent with the description of the polar part of the system (EO blocks and water) as representing a unique, nonhomogeneous phase with a continuous variation of the hydration level along "estuaries" formed by the hydrated EO blocks. The degree of hydration is higher at 295 K compared to 320 K. While qualitative trends are similar for L62 and L64 phases, all hydration values appear drastically reduced in L62 relative to L64 when compared at the same *Z* values. However, comparison on a weight percent basis revealed a much closer similarity. This behavior, observed by us in a number of cases and also by other authors, led us to propose that in L62 a number of PO groups are in the polar regions. The detailed local data support the rationalization of the phase diagrams of Pluronics L62 and L64 in terms of changes in the dimensions of the polar head due to hydration and changes in the curvature of the aggregates due to the hydration gradient in the hydrophilic regions.

## Introduction

In recent years the self-assembly of the triblock copolymers poly(ethylene oxide)-*b*-poly(propylene oxide)-*b*-poly(ethylene oxide), $EO_mPO_nEO_m$ (commercial name Pluronics or Poloxamers), has captivated the attention of researchers. The maturity of the field is reflected in three important reviews,[1] a book chapter,[2] and a recent book.[3] Detailed phase diagrams of binary and ternary systems of several Pluronics have become available,[4−6] and a general understanding of the process of self-assembly in these systems has emerged.[1−7] The Pluronics have often been compared to the much investigated classical nonionic surfactants: For both classes of compounds the micellization in water is determined by the hydrophobic part of the amphiphile and is modulated by the specific interactions of the solvent with the blocks of different polarity. The strong temperature influence on the critical micelle concentration (cmc) is however characteristic only for the $EO_mPO_n$-$EO_m$ copolymers and has been explained by the increasing hydrophobicity of the EO and PO segments as the temperature increases, via the higher weights of the less polar chain conformations.[8]

For nonionic surfactants containing EO groups it is logical to assume that the phase diagram is primarily determined by the dimensions of the polar head and, therefore, dependent on the polymer concentration and the temperature dependence of hydration. This conclusion is well documented for the alkyl-oligo poly(ethylene oxide) series ($C_iEO_j$) surfactants (*i* is the number of carbon atoms in the alkyl group)[9] and seems to be also valid for Pluronics, since the main features of the phase diagrams are similar.[1−6] However, there are few direct determinations of the hydration degrees and profiles in $C_iEO_j$ aggregates,[10] and in Pluronics.[11−13] Information about the *total* hydration in the different lyotropic liquid crystalline (LLC) phases of $EO_{13}PO_{30}EO_{13}$ (L64) and $EO_6PO_{34}EO_6$ (L62) in water has been inferred in recent studies based on small-angle X-ray scattering (SAXS) and $^2H$ NMR data.[4−6]

The nitroxide spin probe electron spin resonance (ESR) method offers a rich source of information on the dynamics, polarity, and self-assembly in surfactants; the problems of probe location and distribution are more complex in the Pluronics compared to the classical surfactants, since the hydrophilic and hydrophobic regions are not as well defined. The complexity of the problem is compounded by the temperature and concentration dependence of the block polarity.

One of us has used spin probe ESR, UV−vis, and fluorescence spectroscopy in a study of reverse micelles (RM) of poly(ethylene oxide) alkyl[14] and alkyl−aryl ethers.[15] The isotropic nitrogen hyperfine splitting, $a_N$, measured in the ESR spectra of a small cationic probe was the quantity used to monitor the polarity in the core

* To whom correspondence should be addressed at the University of Detroit Mercy. E-mail address: SCHLICKS@UDMERCY.EDU.
† Institute of Physical Chemistry.
‡ University of Detroit Mercy.

10.1021/ma980982g CCC: $15.00 
Published on Web 10/10/1998

**Chart 1. Pluronic Triblock Copolymers (a) and CAT$_n$ Spin Probes (b)**

(a) $HO[-CH_2CH_2O-]_m[-CH(CH_3)CH_2O-]_n[-CH_2CH_2O-]_mH$

$(EO_mPO_nEO_m)$

(b) $CH_3(CH_2)_{n-1}N^+(CH_3)_2$–⟨N–O⟩ ($n$=1, 4, 8, 11, 16)

by providing an *effective* local hydration number, $Z_{eff}$, to be compared with the average value, $Z$, determined from the composition of the solution. For the calibration of $a_N$ values as a function of $Z$, poly(ethylene oxide) (PEO)/water mixtures have been used. The results have indicated that the hydration of the EO segments in the ethers is not uniform and decreases from the water core of the reverse micelles. This approach has been extended by using a homologous series of cationic probes 4-(*N*,*N*-dimethyl-*N*-alkyl)ammonium-2,2,6,6-tetramethyl-piperidine-1-oxyl iodides, CAT*n*, with *n*, the number of carbon atoms in the alkyl substituent equal to 1, 4, 8, 11, and 16;[12] the hydration profile in the core of the reverse micelles of L64 at different water contents was deduced from the ESR spectra of these probes.

In a recent study of aqueous $EO_{27}PO_{39}EO_{27}$ (P85) with nonionic and hydrophobic nitroxides such as TEMPO-laurate and TEMPO-hexanoate, very low hydration values have been reported in corona regions near the polar/apolar interface.[13] This behavior is different compared to the ionic surfactants, where the polar part is much smaller and the hydration is uniform.[9,16]

To obtain a more complete picture of the local hydration and to probe the external part of the EO blocks, the use of a homologous series of cationic probes, CAT*n*, presents a series of advantages. *First*, the probe site is determined by the alkyl chain length, and with the nitroxide moiety directly bound to the ionic group, there is no ambiguity regarding its positioning as a result of chain bending, for instance. The problem of probe conformation is especially acute for nitroxide spin probes based on doxylstearic acid. *Second*, with the same nitroxide moiety in the CAT*n* series, $a_N$ values can be directly compared, and using a single calibration curve for all probes in the series, a *polarity profile* can be obtained, as compared to unrelated values based on probes with different structures. *Third*, the CAT*n* probes are located in the more hydrated regions of the corona, which are not examined by the doxyl probes. The utility of the CAT*n* spin probes has been proven in recent studies of L64 reverse micelles,[12] P85 micelles,[13] aqueous solutions of poly(ethylene-*co*-methacrylic acid) (EMAA) ionomers,[17] perfluorinated surfactants,[18] and startburst dendrimers.[19]

In the present study we applied this approach to all phases across the phase diagram in the binary L64/water and L62/water systems, in an attempt to characterize the hydration profiles in the micellar and liquid crystalline phases and to evidence at the molecular level the modifications responsible for phase changes. The copolymers and the probes are shown in Chart 1.

## Experimental Section

**Materials.** The copolymers Pluronics L62 and L64 were BASF products[20] and were used without further purification. Poly(ethylene oxide) (PEO) for calibration was Carbowax200 from Loba Chemie and Carbowax600 from Union Carbide. The spin probes 4-(*N*,*N*-dimethyl-*N*-alkyl)ammonium-2,2,6,6-tetramethyl-piperidine-1-oxyl iodides (CAT*n*), with $n$ = 1, 4, 8, 11, and 16, were purchased from Molecular Probes, Eugene, OR, and used as received.

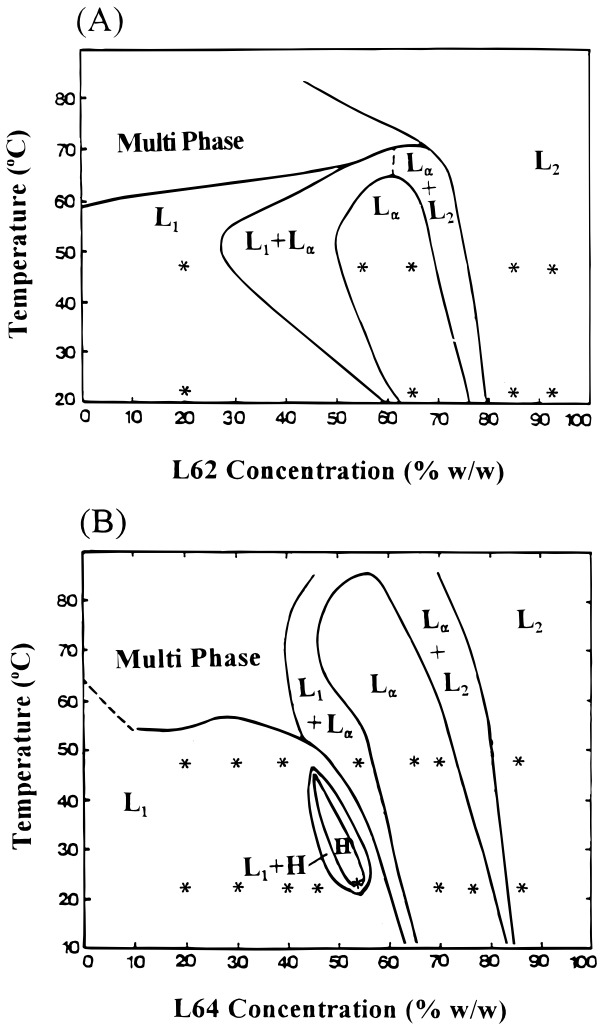


**Figure 1.** Phase diagrams for aqueous $EO_6PO_{34}EO_6$ (Pluronic L62) in (A) and $EO_{13}PO_{30}EO_{13}$ (Pluronic L64) in (B). $L_1$ and $L_2$ are isotropic micellar and reverse micellar phases, respectively, H is the hexagonal phase, and $L_\alpha$ is the lamellar phase. Dotted lines indicate the uncertainty in the phase boundaries (redrawn from ref 6). The compositions investigated in the present work are marked by asterisks.

**Sample Preparation.** The polymer contents were selected to correspond, at 295 K and/or 320 K, to the main phases in the phase diagrams presented in Figure 1. Thus, the polymer concentrations (in % w/w) were 20 (micellar phase $L_1$), 55 (lamellar phase $L_\alpha$ at 320 K), 65 ($L_\alpha$), and 85 and 92 (reverse micellar phase $L_2$) for L62 and 20, 30, 40, and 46 ($L_1$), 54 (hexagonal phase H at 295 K), 65 ($L_\alpha$ at 320 K), 70 ($L_\alpha$), 77 ($L_\alpha$ at 295 K), and 86.1 ($L_2$) for L64; these compositions are indicated by asterisks in Figure 1. The last sample was reported previously in our study of the reverse micelles;[12] the results are included here for comparison with the other phases.

Aqueous solutions of the polymers were prepared in small quantities (≈2 g) by direct weighing of the corresponding amounts of surfactant and bidistilled water, followed by vortex mixing. The mixtures were then gently heated at 320 K for 1 h and left to equilibrate for several days. The hexagonal phase of L64 (54% w/w polymer) formed at room temperature a transparent and optically anisotropic viscous gel, which could only with difficulty be transferred to capillaries. The lamellar phases (65% (w/w) L62, and 70% (w/w) L64) also form transparent and optically anisotropic gels, which flow easier

compared to the hexagonal phase. The lamellar phase obtained at 295 K in the sample containing 77% (w/w) L64 changes to a biphasic region ($L_\alpha + L_2$) at 320 K.

The spin probes were added to the polymer solutions by the following procedure: 10 $\mu$L of a stock solution of the spin probe in ethanol (probe concentration 5 mM) was transferred to a small vial, and the solvent was carefully evaporated, followed by addition of ≈0.2 g of the polymer solution. The samples were mixed with a vortex, heated gently, and left overnight to ensure probe solubilization. In some cases, where control of probe concentration was important, 2.5 $\mu$L of a 10 mM aqueous solution of the probe was added to 0.25 g of each sample (P series); the smaller amount of probe ensured total dissolution, and the small volume of the probe solution eliminated the amount of probe that remained on the sample walls and that was not dissolved. At each temperature the appearance of the liquid crystalline phases was checked by examination between crossed polarizers in the vials and in the sample tubes (Pasteur pipets).

**Calibration of $a_N$.** The ESR spectra of CAT4 in a series of aqueous PEO (Carbowax200) were measured; the calibration curve for $a_N$ previously determined[14] was extended to higher water contents ($Z = 25$). Most $a_N$ values were measured at 320 K, so that rapid tumbling of the probe ensures complete motional averaging of anisotropic effects and more accurate values of $a_N$ can be measured.[21] Similar measurements with Carbowax600 yielded the same calibration curve, within experimental error.

**Quenching Experiments.** These experiments were performed by adding $CuCl_2$ (typically ≈1 mg) to the polymer samples containing the spin probes. An alternative procedure consisted in using a $10^{-2}$ M $CuCl_2$ solution, instead of water, for preparation of the polymer solutions. The two methods led to the same results.

**ESR Measurements.** X-band ESR spectra were measured with a Bruker X-band spectrometer model ECS 106, equipped with the 3240 data system for data acquisition and with the ER4111 VT variable temperature unit. The following parameters were used for spectra acquisition: magnetic field modulation, 100 kHz; microwave power, 2 mW; modulation amplitude, 0.2−0.5 G depending on line width and signal intensity; time constant, 10−40 ms; number of points, 2048; number of scans, 5−10.

**Line Shape Simulations.** For the assignment of some spectral features, comparison with simulated spectra was used. Simulations were accomplished using an updated version of the Freed and Schneider programs for simulation of slow motional spectra.[22]

## Results

X-Band ESR spectra of the CAT*n* spin probes were measured at 295 and 320 K in L64 and L62 aqueous solutions. In some cases lower temperatures were used in order to emphasize special spectral features. Selected ESR spectra for the cationic probes in L64 solutions at 320 and 295 K are presented in Figures 2 and 3, respectively. Corresponding spectra for the L62 system will be discussed.

**ESR Spectra at 320 K.** All spectra (Figure 2) are in the motional narrowing region, with three symmetric signals. The line heights, $h(m_I)$, are in most spectra $h(1) \approx h(0) > h(-1)$, characteristic of rapid isotropic tumbling. The spectra of the smaller and more hydrophilic probes (CAT1, CAT4) exhibit well-resolved proton hyperfine splittings (hfs); the resolution of these small hfs is higher for the low-field lines, as clearly seen in Figure 4, where ESR spectra of CAT4 for three L64 concentrations are shown in greater detail. ESR spectra of CAT4 in neat water, in L64 (54% w/w polymer), and in PEO/water with $Z = 2$ (55% w/w polymer) are compared in Figure 5, in systems containing the same spin probe concentration; clearly the spectral resolution is higher

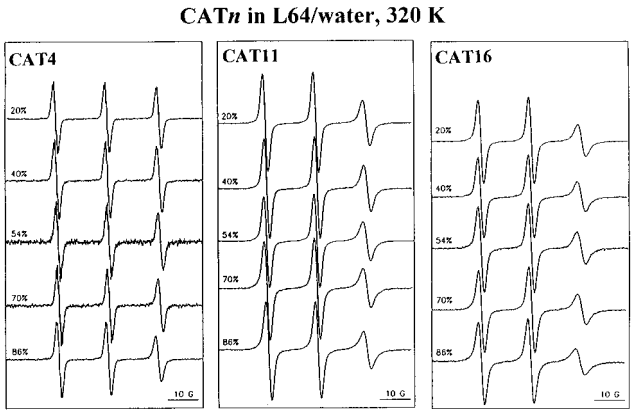


**Figure 2.** Selected X-band ESR spectra at 320 K of CAT*n* spin probes for $n = 4$, 11, and 16 in L64/water solutions for the indicated polymer concentrations in % w/w.

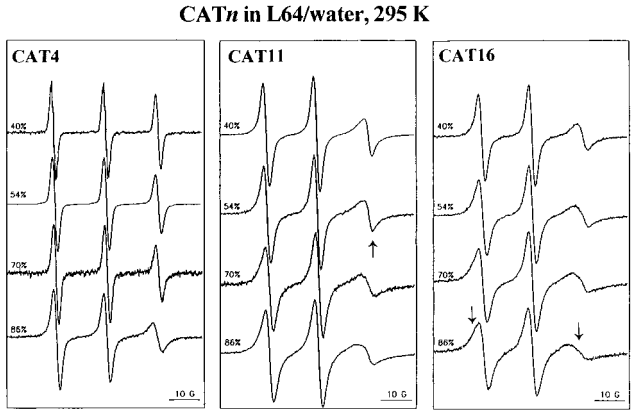


**Figure 3.** As in Figure 2, but ESR spectra measured at 295 K. Upward arrow (for CAT11) points to a superposition of two spectral components; downward arrows (for CAT16) show line broadening due to incomplete motional averaging ("dynamic effects").

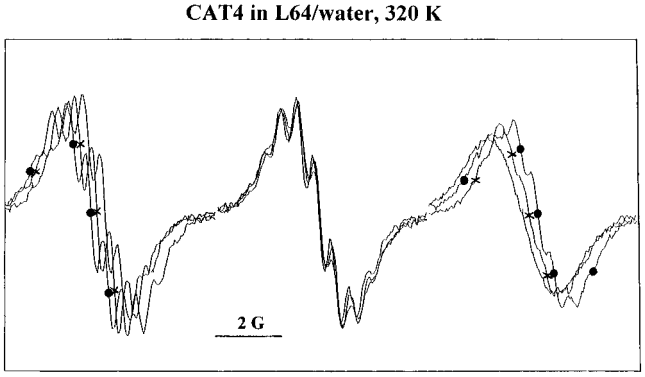


**Figure 4.** Horizontally expanded ESR spectra of CAT4 at 320 K in L64 solutions containing 70%, 54% (×), and 40% (●) (w/w) L64.

for the probe in the copolymer/water and PEO/water samples, compared to neat water. Moreover, we found that the spectral resolution *increases* in the series 20% to 40% and to 54% w/w L64 solutions; this was checked on the P series of samples (vide supra), in which the spin probe was introduced in carefully controlled, equal quantities. A similar effect was detected for L62 solutions when comparing solutions with 20 and 55% (w/w) polymer.

The viscosity dependence of the line width of the proton signals, $W_H$, due to the relaxation effects that result from spin-rotation interaction and motional av-

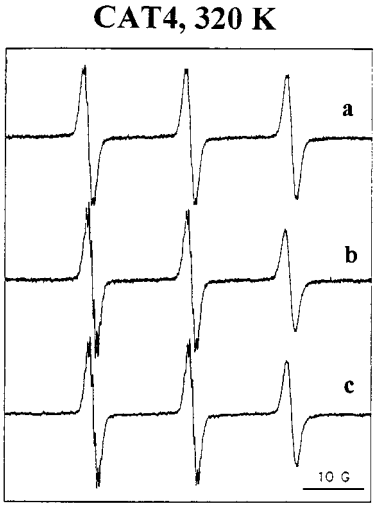


**Figure 5.** ESR spectra at 320 K of CAT4 (series P, see Experimental Section) in neat water (a), in L64 54% (w/w) (b), and in PEO/water with $Z = 2$ (55% (w/w) PEO) (c).

eraging of the $g$ and $^{14}N$ hyperfine tensors can be described as in eq 1,[23]

$$W_H = \frac{K_1 k_B T}{\eta} + \frac{K_2 \eta}{k_B T} + K_3 \qquad (1)$$

where $k_B$ is the Boltzmann constant, $\eta$ is the viscosity, $T$ is the temperature, and $K_1$, $K_2$, and $K_3$ are constants. Joliceur et al. found this equation to account reasonably well for the viscosity dependence of $W_H$ for TEMPO as the spin probe in water−glycerol mixtures.[24] The observed trend to narrower proton line widths as $\eta$ increases is expected in the regime in which the spin−rotation relaxation mechanism, reflected by the first term of eq 1, is dominant. The increased resolution for CAT*n* probes in L62 and L64 solutions compared to neat water can be explained by assuming intercalation of the spin probes in polymer aggregates where the motional restrictions are significant. For CAT8, CAT11, and CAT16 the proton hfs are not resolved, as seen clearly in Figures 2. For these large radicals located in the viscous regions of the aggregate interior complete averaging of the anisotropic effects does not occur even at 320 K, and the residual line widths are comparable or larger than the proton splittings.

The resolution of the ESR spectra measured for the small cationic probes (CAT1 and CAT4), together with the simple line shapes measured for all probes at 320 K (Figure 2) and with the line width dependence on the viscosity, indicates the presence of one spectral component, which reflects the association of the probes with the polymer aggregates.

**ESR Spectra at 295 K.** These spectra reflect reduced rates of tumbling along certain axes for all spin probes. As the polymer concentration increases, the line heights for CAT1, CAT4 and CAT8 change from $h(1) \approx h(0) > h(-1)$, to $h(1) > h(0) > h(-1)$, the latter order specific of preferential rotation around the long molecular axis, parallel to the N−O bond; for CAT11 and CAT16 the line heights order becomes $h(0) > h(1) > h(-1)$. The simulated spectra shown in Figure 6 indicate that a small change of the tilt angle between the long molecular axis (rotation axis) and the nitrogen $2p\pi$ orbital, from 50° to 60°, may produce this effect.

For some of the largest probes in the more concentrated polymer samples (CAT11 and CAT16 in L64 55−86% (w/w), and CAT16 in L62 65−92% (w/w)), the spectra present increasingly asymmetric lines, as shown in Figure 3 by downward arrows for CAT16 at high L64 content. The same line shapes were also detected for CAT16 in solutions of Carbowax200 and were simulated with *one* spectral component only, suggesting that this line shape is due to incomplete motional averaging of the spectral anisotropy ("dynamic effects"). This result is not surprising for the most hydrophobic probe, CAT16, which is expected to intercalate deeply in the polymer aggregates.

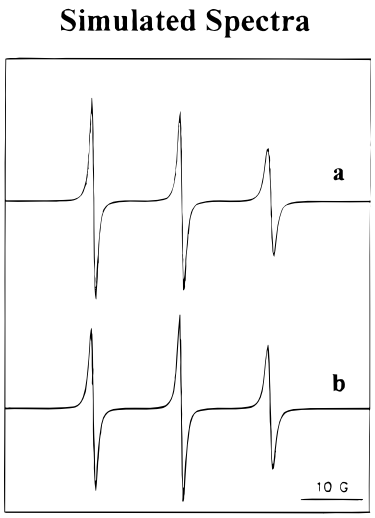


**Figure 6.** Simulated spectra, with the following parameters: $g_{xx} = 2.0089$, $g_{yy} = 2.0073$, $g_{zz} = 2.0036$, $A_{xx} = 6.1$ G, $A_{yy} = 5.9$ G, $A_{zz} = 32.6$ G,[30] diffusion tensor components $R_\perp = 1 \times 10^8$ $s^{-1}$, $R_\parallel = 1 \times 10^{10}$ $s^{-1}$, coefficient of the ordering potential $\lambda = 0.5$, line width 0.5 G, and tilt angle $\theta = 60°$ (a) and $\theta = 50°$ (b).

Some of the spectra shown in Figure 3 suggest a superposition of two components, for instance in the case of CAT11 in L64 (54% (w/w) polymer), as shown by the upward arrow in Figure 3. The appearance of *two* components suggests that the exchange rate between the two sites at 295 K is slow on the ESR time scale ($\nu_{ex} < 10^8$ $s^{-1}$). Because the major site detected is clearly associated with probes located in the polymer aggregates, the second site is most likely due to the location of the probe in water; the distribution of the probe between the two sites is expected to depend on the probe concentration. To check this possibility, two series of samples were prepared for CAT11 in L64 solutions (70 and 54% (w/w) polymer), with probe concentrations of $1 \times 10^{-4}$ and $2 \times 10^{-4}$ M, respectively. ESR spectra in the 70% (w/w) L64 solution at 280, 295, and 320 K are shown in Figure 7A. For the higher probe concentrations (upper spectrum at each temperature) the spectral overlap is clearly visible on the high-field line, especially at 280 and 295 K. The spectrum in Figure 7B was obtained by subtracting the spectrum of the probe in neat water at 295 K from the spectrum of the more concentrated probe sample at the same temperature and is identical with that of the more dilute probe sample.

The effect of $CuCl_2$ on the line shapes, shown in Figure 8 for spectra measured at 295 K, provided additional evidence for the presence of *two* spectral components in some solutions and for the proposed locations of the probes. The composite signal at high field shown in spectrum a of Figure 8 for CAT11 in L64 (70% w/w polymer) changes on $CuCl_2$ addition due to

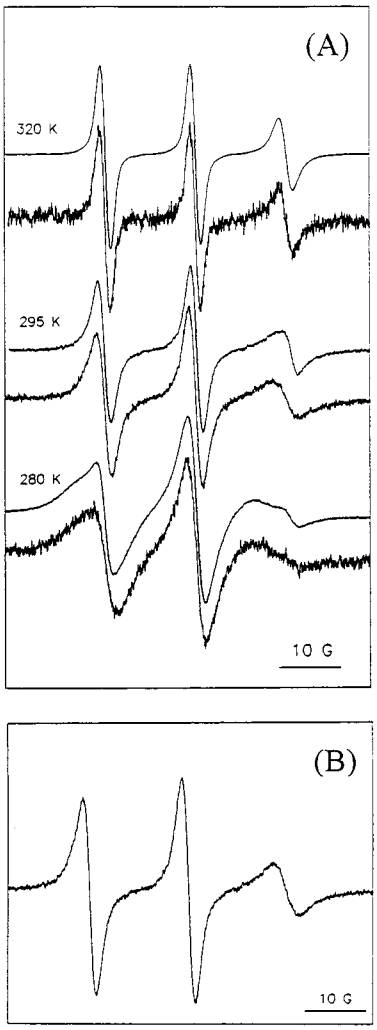


**Figure 7.** (A) X-Band ESR spectra of CAT11 in L64 (70% (w/w) polymer) at the indicated temperatures and at two probe concentrations: $4 \times 10^{-4}$ M (upper trace) and $2 \times 10^{-4}$ M (lower trace) at each temperature. (B) The ESR spectrum obtained after subtraction of the spectrum at 295 K of CAT11 in neat water from the spectrum at 295 K of the same probe at the higher concentration in L64 (70% (w/w) polymer).

the disappearance of the signal for the probe in water (spectrum b). The broader signal from the probe intercalated in the aggregates is not affected because the long probe is located deep in the aggregates where the hydration is low, and therefore the access of $CuCl_2$ is limited. For CAT1, CAT4, and CAT8 the proton resolution is almost completely lost, but the lines are symmetric. The probes have higher mobility due to their smaller sizes but also due to their location toward the exterior of the aggregate. Spectrum c of CAT8 in L64 (70% (w/w) polymer) changes to spectrum d on $CuCl_2$ addition; the nonselective, general line-broadening effect is clearly seen. This fact represents experimental evidence for the location of the probe in well-hydrated sites, and excludes the possibility of spectral overlap from sites with different degrees of hydration.

**Values of $a_N$.** The $a_N$ values are reported in Tables 1 and 2, as a function of the water content expressed as *Z*. Due to the line asymmetry discussed above, correct $a_N$ values cannot be read from the spectra measured at 295 K in some cases. The data at 295 K given in the tables resulted from dilute samples or after spectral subtraction of the corresponding spectrum of

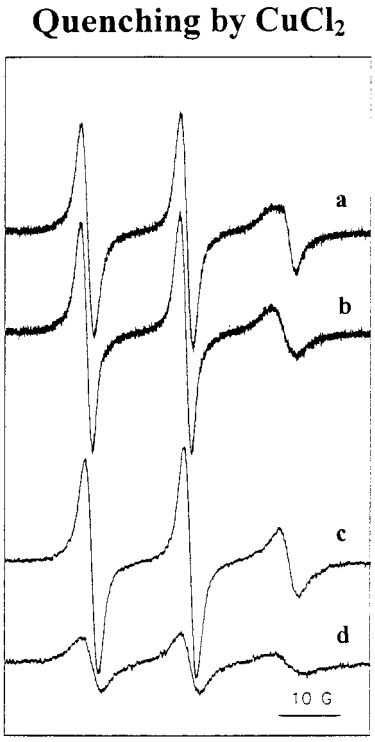


**Figure 8.** Quenching experiments at 295 K of CAT*n* spin probes in L64/water. Spectra a and c are the original ESR spectra for CAT11 and CAT8, respectively, in L64 (70% (w/w) polymer); spectra b and d are the corresponding spectra after addition of $CuCl_2$ (see text).

**Table 1. $^{14}$N Hyperfine Splittings, $a_N$ (G), of CAT*n* Probes in L64/Water[a]**

| phase | L64 (wt %) | *Z* | CAT1 | CAT4 | CAT8 | CAT11 | CAT16 |
|---|---|---|---|---|---|---|---|
| | | | 320 K | | | | |
| $L_1$ | 20 | 25 | 16.65 | 16.62 | 16.50 | 16.31 | 16.11 |
| $L_1$ | 30 | 14.5 | 16.60 | 16.57 | 16.40 | 16.21 | 16.09 |
| $L_1$ | 40 | 9.3 | 16.55 | 16.53 | 16.32 | 16.21 | 16.09 |
| $L_\alpha + L_1$ | 54 | 5.2 | 16.50 | 16.48 | 16.23 | 16.14 | 16.00 |
| $L_\alpha$ | 65 | 3.3 | 16.37 | 16.35 | 16.20 | n | 16.04 |
| $L_\alpha$ | 70 | 2.7 | 16.33 | 16.25 | 16.22 | 16.12 | 16.05 |
| $L_2$ | 86 | 1.0 | 16.08 | 16.00 | 15.95 | 15.90 | 15.80 |
| | | | 295 K | | | | |
| $L_1$ | 20 | 25 | | 16.66 | 16.62 | 16.50[b] | 16.25[b] |
| $L_1$ | 30 | 14.5 | | 16.60 | 16.57 | 16.29[b] | 16.21[b] |
| $L_1$ | 40 | 9.3 | | 16.58 | 16.51 | 16.35[b] | 16.20 |
| $L_1$ | 46 | 7.3 | 16.55 | 16.55 | 16.40 | n | 16.15 |
| H | 54 | 5.2 | 16.55 | 16.50 | 16.43 | 16.30[b] | 16.14 |
| $L_\alpha$ | 70 | 2.7 | 16.42 | 16.38 | 16.27 | a | a |
| $L_\alpha$ | 77 | 1.9 | 16.20 | 16.26 | 16.16 | a | a |
| $L_2$ | 86 | 1.0 | 16.20 | 16.09 | 15.90 | a | a |

[a] Key: n, not performed; a, dynamic effects. [b] After subtraction of the ESR spectrum for the probe in neat water.

the probe in neat water and represent therefore $a_N$ values for the spin probes associated with the polymer aggregates.

A decrease of $a_N$ in the homologous series of CAT*n* probes when *n* increases is clearly deduced from the spectra and the data in Tables 1 and 2. The $a_N$ values range between the value in neat Carbowax200 ($a_N$ = 15.65 G) and values close to, but lower than, the value in water ($a_N$ = 16.80 G). The data also indicate that as the polymer concentration increases and/or the probe "tail" increases, the $a_N$ values decrease. The more limited data given at 295 K show an increase of $a_N$ values compared to those measured at 320 K. The effect

**Table 2. $^{14}$N Hyperfine Splittings, $a_N$ (G), for CAT*n* Probes in L62/Water**

| phase | L62 (wt %) | *Z* | CAT 1 | CAT 4 | CAT 8 | CAT 16 |
|---|---|---|---|---|---|---|
| | | | 320 K | | | |
| $L_1$ | 20 | 46.3 | | 16.64 | 16.51 | 16.08 |
| $L_\alpha$ | 55 | 9.5 | 16.54 | 16.48 | 16.20 | 16.00 |
| $L_\alpha$ | 65 | 6.2 | 16.39 | 16.34 | 16.18 | 16.14 |
| $L_2$ | 85 | 2.0 | 16.13 | 16.09 | 15.97 | 15.83 |
| $L_2$ | 92 | 1.0 | 15.90 | 15.86 | 15.74 | 15.72 |
| | | | 295 K | | | |
| $L_1$ | 20 | 46.3 | | 16.64 | 16.61 | 16.33 |
| $L_\alpha$ | 65 | 6.2 | 16.41 | 16.43 | 16.28 | 15.95 |
| $L_2$ | 85 | 2.0 | 16.25 | 16.11 | 16.04 | *a* |
| $L_2$ | 92 | 1.0 | 16.05 | 15.96 | 15.76 | *a* |

[a] Dynamic effects.

is especially important for those probes in the intermediate hydration region: CAT4 in L64 (70% (w/w)) and L62 (65% (w/w)), CAT8 in L64 (54% and 40%) and L62 (65% (w/w)). The increase of $a_N$ as the polymer concentration decreases is specific for each probe.

**Effective Hydration $Z_{eff}$.** Calibration of $a_N$ values in terms of the ratio $Z$ = [water]/[EO] was done using the calibration curve of CAT4 in Carbowax200/water mixtures. In Figure 9 we present the $a_N$ vs $Z$ curves at 320 and 295 K for all probes in L64 solutions, together with the calibration curve. The local hydration values, $Z_{eff}$, corresponding to the $a_N$ values of each probe, were extracted from the calibration curve. The $Z_{eff}$ values as a function of $Z$ are presented in Figures 10 (for L64) and 11 (for L62), at 320 and 295 K for both copolymers.

## Discussion

In a simplified model, the Pluronic aggregates in water can be described as consisting of a polar part made of the EO blocks and water and an apolar part represented by the PO block. In this section we will describe the location of the probes and the hydration gradient in L64 and L62 solutions deduced by analyzing data for the CAT*n* spin probes in PEO/water solutions, and in the L64/water and L62/water systems, and will compare the results with the most recent and complete study of these Pluronics based on SAXS and $^2$H NMR.[6]

**Sites Reported by the Spin Probes.** In PEO/water mixtures that are homogeneous at the molecular level, all CAT*n* spin probes are expected to exhibit spectra with the same $a_N$ values within experimental precision (±0.01 G), irrespective of *n*. This behavior was experimentally confirmed. In addition, no significant temperature effect on $a_N$ was detected.[19] The $a_N$ variation with water content is described by the calibration curve given in Figure 9.

In the Pluronics/water samples, however, each spin probe indicates a different polarity, which decreases in all samples when *n* increases. For amphiphilic spin probes such as CAT*n*, the spectrum in aqueous solutions of surfactants (above cmc) is expected to be influenced by the equilibrium between isolated spin probes and spin probes associated with surfactant aggregates. The line shapes depend on the frequency of the chemical exchange rate, $\nu_{ex}$, of the probe between the bulk and the micellar environment, compared to $\Delta\omega$, the separation (in rad/s) between the signals of the probe in the two sites. The typical difference in $a_N$ for the spin probes in neat water and PEO solutions is ≈1 G; therefore $\Delta\omega \approx 2 \times 10^7$ rad/s. The exchange rate depends on the structures of the surfactant and the radical and on the temperature. Nakagawa and Jizomoto found that in a homologous series of neutral radicals the residence time in micelles of sodium dodecyl

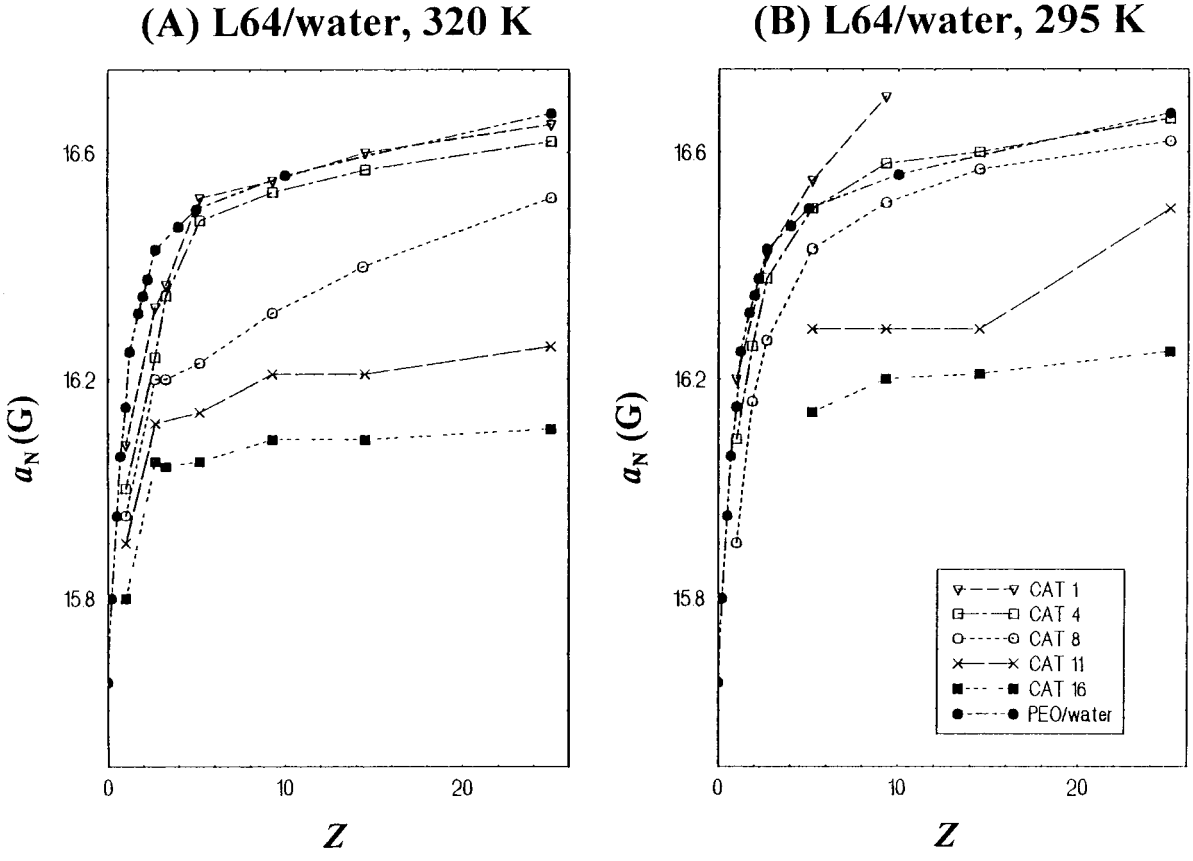


**Figure 9.** Plot of $a_N$ vs $Z$ for the CAT*n* series in L64/water and for CAT4 in PEO/water at 320 K in (A) and at 295 K in (B).

sulfate and homologous surfactants increased by a factor of 3 for each added $-CH_2-$group.[25] Hydrophobic probes with long alkyl chains, for instance TEMPO-laurate and TEMPO-hexanoate, report on the interior regions of the micelles and have a slow exchange rate.[13] In these cases the two spectra have very different $a_N$ and correlation times $\tau_c$, and the overlap leads to the splitting of at least one line, usually the high field signal ($m_I = -1$). Selective quenching of the water spectrum with $CuCl_2$ and subtraction of the spectrum in water are effective ways to recovering the ESR spectra of the probes located in the aggregates. This is also true for the more hydrophobic probes such as CAT11 and CAT16.

Thus, for the higher members of the series, CAT16, CAT11, and CAT8 (the last one for L64 concentrations ≥50% (w/w)), the data in Table 1 correspond to probes in the aggregates and their $a_N$ values reflect local hydration values. Examination of these $a_N$ values and the corresponding effective hydration, $Z_{eff}$, shows very little hydration, with saturation of hydration at about 70% (w/w) L64, in the lamellar phase.

To probe the external regions, however, the more hydrophilic probes are essential. General considerations indicate that CAT1, CAT4, and CAT8 have a higher water solubility; therefore significant partitioning in water is expected, especially at higher probe and lower surfactant concentrations. It is also reasonable to consider that these probes are located in highly hydrated sites in the aggregate, with spectral parameters similar to those of water. The ESR spectra with well-resolved proton splittings and symmetry relative to the line center observed for these probes, as seen clearly in Figure 4, cannot result from overlap of water and aggregate spectra (the last ones with different $g$ and $a_N$ values, depending on the aggregate type). Slight differences in the overlap would be easily identified due to distortions of the proton hfs pattern. In these cases cooling to 280 K does not reveal line asymmetries and $CuCl_2$ produces no selective quenching, only an overall line broadening. Thus, it is evident that these spectra do not represent spectral overlaps, but averages. A rapid exchange rate is expected for these smaller radicals. If the observed spectra originated from rapid averaging on the ESR time scale ($\approx 10^{-8}$ s) of two or more different probe locations, distinct spectra would appear when using a shorter detection time scale. However, UV−vis absorption spectroscopy (time scale $\approx 10^{-14}$ s) of probes with similar hydrophilic character and polarity dependence of the spectral parameters and introduced into the same systems, present unique, narrow lines, pointing to a narrow distribution of probe locations.[26] Consequently, the measured $a_N$ values should be interpreted in these samples as *local averages* over a region of the corona and the water trapped between polymer chains, at different radial depths in the aggregates. With Pluronics the problem appears more complex than with the ionic surfactants, due to the extended polar head. The corona can be described as a nonuniform phase with water between polymer chains. The long polymer chains are extending from the aggregates into water and along the "estuaries" formed, and the water/EO ratio has a continuous variation from zero (close to the polar/apolar interface) to higher values as the distance from the interface increases.

In a recent paper Lüsse and Arnold measured spin−lattice and spin−spin relaxation times of $^1H$ and $^2H$ nuclei by NMR and deduced that the number of water molecules bound to each EO group is unity, using a model of fast exchange between bound and unbound water molecules.[27] To account for phase changes as a function of surfactant concentration, however, a different quantity has to be considered: It must be recognized that more than one water molecule per EO unit contributes to the polar head volume; from this point of view "hydration" implies water molecules confined between the polymer chains, in addition to hydrogen-bonded water. Our data are therefore closer to self-diffusion data,[9b] which measure *all* the water molecules that migrate with the micelle.

Having established the way hydration and $Z_{eff}$ values are interpreted, it is interesting to examine the variation of the degree of hydration and the hydration gradient along the EO segments in the different phases, at the two temperatures.

**Hydration Gradient in L64.** Examination of the $Z_{eff}$ values presented in Figure 10A together with the phases present and the $Z$ values of the solutions studied (Table 1) indicates that at 320 K a polarity gradient is already established in the reverse micelles ($L_2$ phase); the hydration level is low but increases steeply along the EO blocks, up to the appearance of the lamellar phase represented by the solution containing 70% (w/w) L64 ($Z = 2.7$). With further water addition, the inner layers of the aggregates seem to have reached saturation, as the $Z_{eff}$ values indicated by CAT16, CAT11, and CAT8 remain almost unchanged. Water accumulates only in the external part of the lamellae, as clearly seen from the large increase of hydration shown by CAT4 and CAT1 up to 54% (w/w) L64 ($Z = 5.2$). Eventually the hydration of the external regions leads to the phase change from lamellar to micellar. Above $Z \approx 5$, in the $L_1$ phase, the increase in the hydration is less steep.

The data are significantly different at 295 K, Figure 10B. The first observation is that all hydration values are higher at 295 K compared to 320 K. While CAT11 and CAT16 indicate saturation of the inner regions starting from 70% (w/w) L64 (at a slightly higher hydration level compared to 320 K), in the intermediate regions (revealed by CAT4 and CAT8) a steep increase in hydration continues up to 40% (w/w) polymer ($Z = 9.3$). In accord with these data, the phase change from lamellar to hexagonal occurs at 295 K at 54% (w/w) L64 ($Z = 5.2$), while at 320 K at the same concentration the lamellar phase is maintained.

**Hydration Gradient in L62.** The $a_N$ data presented in Tables 1 and 2 for the two block copolymers show a similar qualitative evolution with polymer concentration and with temperature. When comparing the two surfactants at the same water to EO ratio (equal $Z$ values), hydration appears strongly reduced in L62 vs L64, especially in the intermediate regions of the aggregates, at both temperatures; this conclusion emerges by comparing Figures 10 and 11, and Tables 1 and 2. However, if the two systems are compared on % w/w basis, the hydration profiles of L64 and L62 appear very similar, as seen by comparing parts a and b of Figure 12. This is surprising, taking into consideration the block composition of the two polymers: the EO block represents 40% (w/w) in L64 and only 20% (w/w) in L62, so that in solutions of equal composition in % w/w, $Z$ is twice as high in L62 compared with L64.

Some literature data also show a similarity for the two systems when compared on a weight percentage basis: (i) the phase boundaries of the $L_2$ phase[28] and of

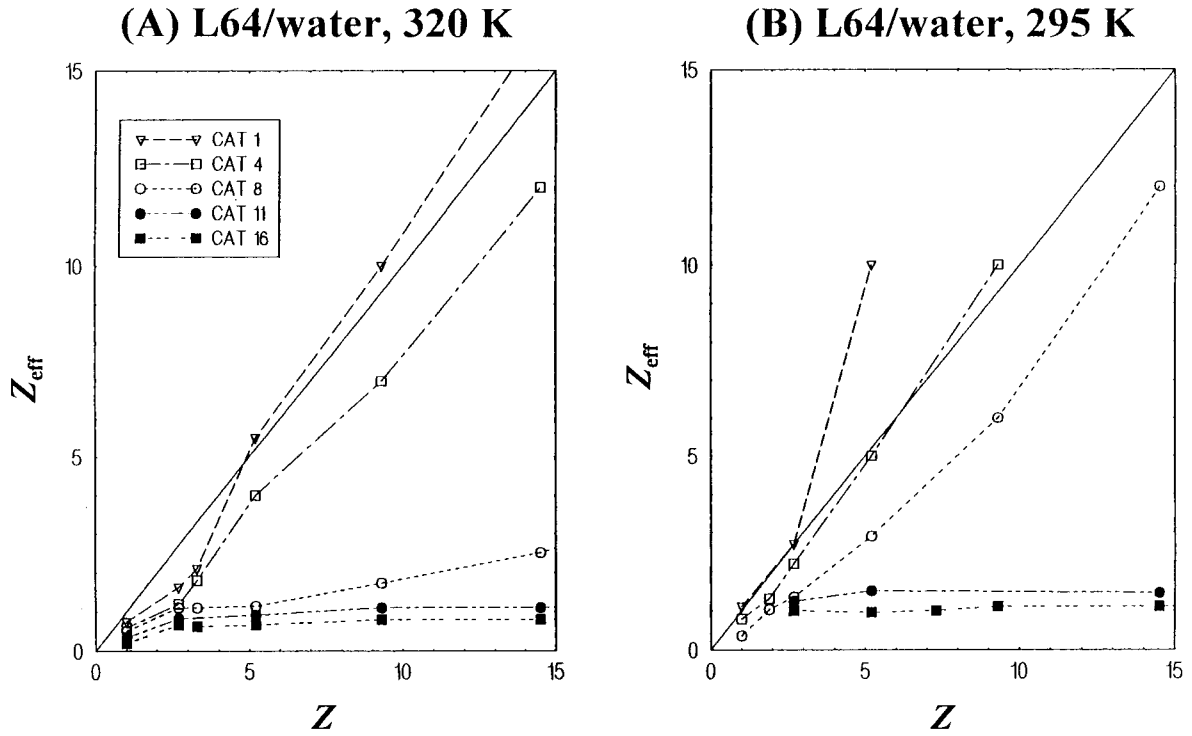


**Figure 10.** Effective degrees of hydration, $Z_{eff}$, *vs* $Z$, for L64/water at 320 K in (A) and at 295 K in (B); the $Z_{eff}$ values are obtained from the $a_N$ value for each probe, by reading the corresponding $Z$ value from the calibration curve based on CAT4 in aqueous PEO in Figure 9 (see text). Data were plotted for $Z$ values in the range 0−15 (not for $Z = 25$) to emphasize changes occurring at low hydration levels.

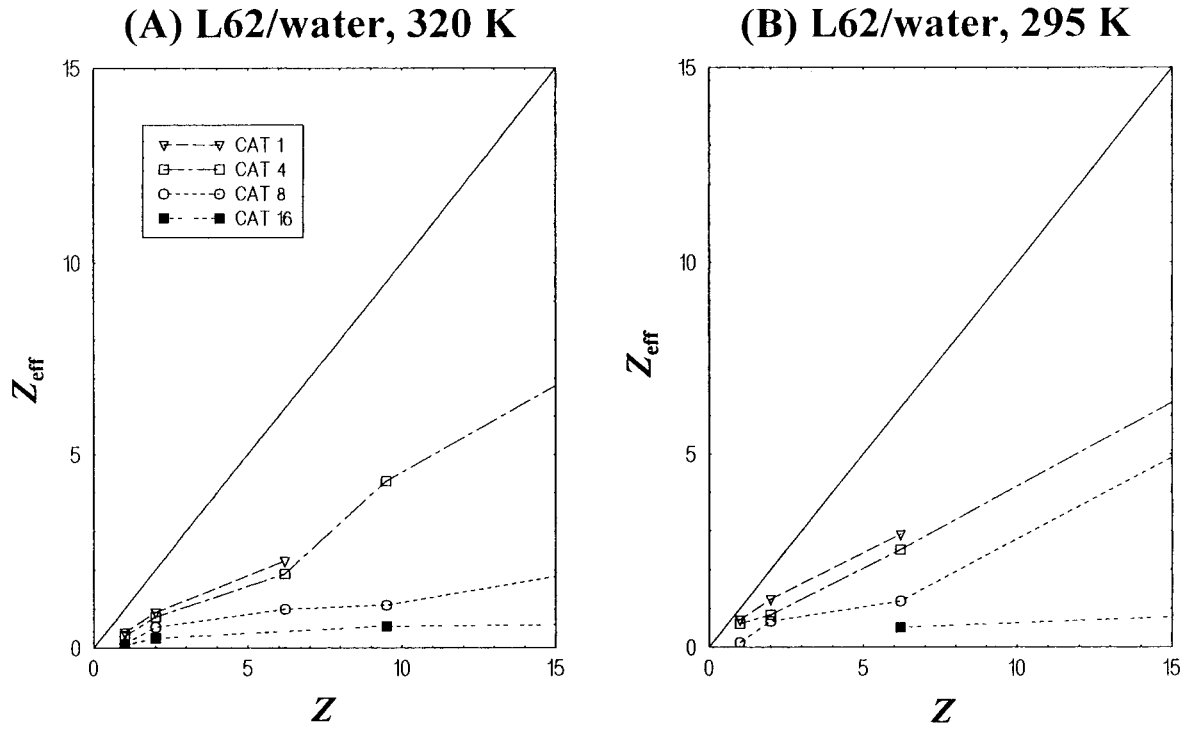


**Figure 11.** Effective hydration degrees, $Z_{eff}$, vs $Z$ for L62/water at 320 K in (A) and at 295 K in (B). For details see previous caption.

the lamellar phase[6] are similar for the two surfactants; (ii) reverse micelles of L64 and L62 in 34.5% xylene solution are formed at a minimum amount of water correponding to $Z = 0.2$ for L64 and $Z = 0.4$ for L62, or 1.1% (w/w) in both cases;[29] the reverse micelles formed dissolve the same maximum quantity of water (in % w/w), corresponding to $Z = 2$ for L64 and $Z = 4$ for L62;[28,29] (iii) the quadrupole splitting of deuterons in $^2$H NMR spectra indicate water saturation in the lamellar phases at $Z = 5$ for L62 and at $Z = 2.7$ for L64 (both at 70% (w/w) polymer);[6] (iv) the interfacial area per EO block is reduced by only ≈10% for L62 compared to L64 in 64% (w/w) solutions.[6] Thus, L62 seems to behave as if it had the same number of EO units as L64. This effect could be due to the large difference in the sizes of the two blocks, which can cause strong packing

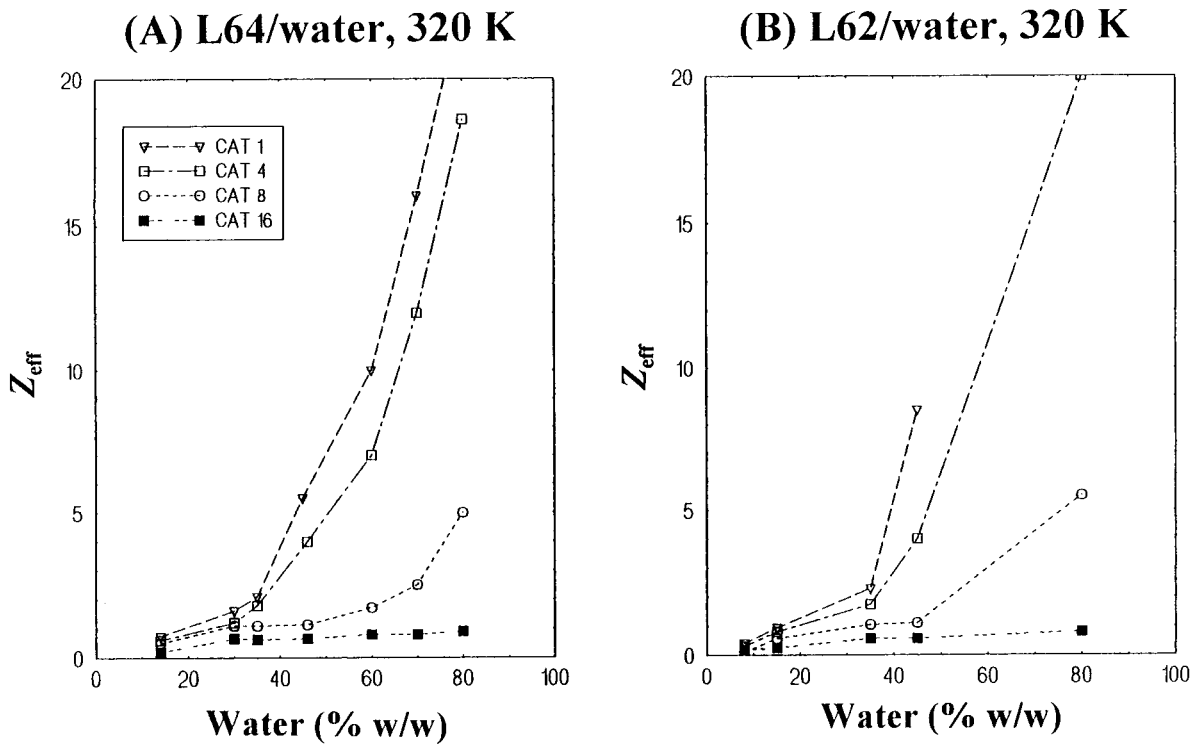


**Figure 12.** Effective hydration degrees, $Z_{eff}$, at 320 K vs water content expressed as % w/w for L64/water in (A) and for L62/water in (B).

restrictions. Involving a few PO units into the polar part might be possible due to the small difference in hydrophilic/hydrophobic character of the two blocks. Indeed, fluorescent probes localized at the EO/PO interface region of reverse micelles in the L62/*o*-xylene/water system indicate slightly lower polarities compared to the similar L64 micelles, while in the polar regions of the core the two systems are similar.[29]

**Comparison with SAXS Data.** The lattice parameter of the lamellar and hexagonal LLC phases of L64 and other Pluronic block copolymers have been calculated by SAXS as a function of temperature and polymer concentration in water.[6] Assuming a sharp interface between the polar and apolar domains and based on simple geometric considerations, the lattice parameter $d$, the apolar domain thickness $\delta$, and the interfacial area per EO block were deduced. It is interesting to see whether and how do these "global" structural characteristics of the LLC aggregates correlate with the variations of the hydration profiles based on ESR spectra of the spin probes in the present study.

At 298 K, with decrease of polymer concentration, the thickness of the polar domain (the difference between the lattice parameter $d$ and the apolar thickness $\delta$) and the interfacial area per EO block in the lamellar phase were found to increase for both L62 and L64 (Figure 4 of ref 6). The corresponding observation in this spin probe study is the increase of hydration in the outer and intermediate regions (reflected in data for CAT1, CAT4, and CAT8) of the lamellae, while a constant hydration in the inner regions (reflected in data for CAT11 and CAT16) is maintained. Raising the temperature for the same samples leads to a decrease in the polymer interfacial area (Figure 5 of ref 6), an effect that was attributed to the dehydration of the polymer molecules. Indeed, the spin probe study reports a reduced hydration along the normal to the interface, with special emphasis at medium levels reported by CAT8. SAXS data also show that for L64 at 298 K the interfacial area per EO group has a significantly higher value in the hexagonal phase (100−107 Å$^2$)[4b] compared to the lamellar phase (80−87 Å$^2$).[6] Our data parallel these results and add more details, by indicating an increase of hydration in the hexagonal vs lamellar phase at the outer levels (CAT1 and CAT4) and even more so at the intermediate levels (CAT8), while the inner levels are not affected. This process leads to curvature changes and to a different packing, from lamellae to cylindrical or spherical micelles.

An estimate of the scale of the hydration gradient reported by the spin probes can be obtained from the SAXS data for the lamellar phase:[6] between 25 and 60 °C the lattice parameter $d$ is in the range 77−82 Å for L64 and 77−85 Å for L62; the thickness $\delta$ of the apolar part is in the range 30−40 Å for L64 and 40−50 Å for L62. The length of the two EO blocks is therefore expected to be ≈40 Å in both L64 and L62. The scale of the polarity and hydration level in the corona explored by the CAT*n* probes is therefore similar, ≤20 Å, in both systems.

## Conclusions

Aqueous solutions of $EO_{13}PO_{30}EO_{13}$ (Pluronic L64) and $EO_6PO_{34}EO_6$ (Pluronic L62) were investigated in the micellar, liquid crystalline, and reverse micellar phases by a homologous series of cationic nitroxide spin probes, CAT*n*, where *n* is the number of carbon atoms in the alkyl substituent. The main objective was to measure the local polarity and the polarity gradient in the polar regions of the self-assembled polymer aggregates. The isotropic hyperfine splitting from the $^{14}N$ nucleus, $a_N$, was the polarity-sensitive parameter, and $a_N$ values were translated into *effective* local hydration values, $Z_{eff}$, based on ESR of the cationic spin probes in PEO/water mixtures as a function of the water content expressed as $Z = [H_2O]/[EO]$ (molar ratio).

The results are consistent with the description of the polar part of the system (EO blocks and water) as representing a unique, nonhomogeneous phase with a continuous variation of the hydration degree along the hydrated EO segments. The degree of hydration is higher at 295 K compared to 320 K. The detailed local data support the rationalization of the phase diagrams of Pluronics L62 and L64 in terms of changes in the dimensions of the polar head due to hydration and changes in the curvature of the aggregates due to the hydration gradient in the hydrophilic regions.

While qualitative trends are similar for L62 and L64 phases, all hydration values appear drastically reduced in L62 relative to L64 when compared at the same *Z* values. However, comparison on a weight percent basis reveals a much closer similarity. This behavior, observed by us in a number of cases and also by other authors, led us to propose that in L62 a number of PO groups are in the polar regions; this effect could be a result of the large difference in the size of the PO and EO blocks in L62.

**Acknowledgment.** This study was supported by the Polymers Program of the National Science Foundation and by the National Research Council Program for Collaboration in Basic Science and Engineering (COBASE) between US and Romania in support of the stay in Detroit of Agneta Caragheorgheopol.

## References and Notes

(1) (a) Alexandridis, P.; Hatton, T. A. *Colloid Surf., A* **1995**, *96*, 1. (b) Almgren, M.; Brown, W.; Hvidt, S. *Colloid Polym. Sci.* **1995**, 273. (c) Alexandridis, P. *Curr. Opin. Colloid Interface Sci.* **1997**, *2*, 478.

(2) Chu, B.; Zhou, Z. In *Nonionic Surfactants*; Marcel Dekker: New York, 1996; Chapter 3, p 67.

(3) *Amphiphilic Block Copolymers: Self-Assembly and Applications*, Alexandridis, P., Lindman, B., Eds.; Elsevier: Amsterdam, 1997.

(4) (a) Zhang, K.; Khan, A. *Macromolecules* **1995**, *28*, 3807. (b) Alexandridis, P.; Olsson, U.; Lindman, B. *Macromolecules* **1995**, *28*, 7700.

(5) Alexandridis, P.; Olsson, U.; Lindman, B. *J. Phys. Chem.* **1996**, *100*, 280. This study presents the phase diagram of a *reverse* Pluronic (EO block in the middle) in water−oil mixtures.

(6) Alexandridis, P.; Zhou, D.; Khan, A. *Langmuir* **1996**, *12*, 2690. The phase diagram for L64 is more accurate and detailed compared to that published previously (ref 4a).

(7) Wu, W.; Zhou, Z. K.; Chu, B. *Macromolecules* **1993**, *26*, 2117. Wu, W.; Chu, B. *Macromolecules* **1994**, *27*, 1766. (c) Zhou, S.; Chu, B. *J. Polym. Sci., Part B: Polym. Phys.* **1998**, *36*, 889.

(8) (a) Andersson, M.; Karlstrom, G. *J. Chem. Phys.* **1985**, *89*, 4957. (b) Linse, P. *Macromolecules* **1993**, *26*, 4437. (c) Hurter, P. N.; Scheutjens, J. M. H. M.; Hatton, T. A. *Macromolecules* **1993**, *26*, 5030.

(9) (a) Medhage, B.; Almgren, M.; Alsins, J. *J. Phys. Chem.* **1993**, *97*, 7753. (b) Nilsson, P.-G.; Wennerstrom, H.; Lindman, B. *J. Phys. Chem.* **1983**, *87*, 1977.

(10) Baglioni, P.; Bongiovanni, R.; Rivara-Minten, E.; Kevan, L. *J. Phys. Chem.* **1989**, *93*, 5574.

(11) Malka, K.; Schlick, S. *Macromolecules* **1997**, *30*, 456.

(12) Caragheorgheopol, A.; Pilar, J.; Schlick, S. *Macromolecules* **1997**, *30*, 2923.

(13) Caragheorgheopol, A.; Caldararu, H.; Dragutan, I.; Joela, H.; Brown, W. *Langmuir* **1997**, *13*, 6912.

(14) Caldararu, H.; Caragheorgheopol, A.; Vasilescu, M.; Dragutan, I.; Lemmetyinen, H. *J. Phys. Chem.* **1994**, *98*, 5320.

(15) (a) Caldararu, H.; Caragheorgheopol, A.; Dimonie, M.; Donescu, D.; Marinescu, M. *J. Phys. Chem.* **1992**, *96*, 7109. (b) Caragheorgheopol, A.; Bandula, R.; Caldararu, H.; Joela, H. *J. Mol. Liq.* **1997**, *72*, 105.

(16) Mortensen, K.; Brown, W. *Macromolecules* **1993**, *26*, 4128.

(17) Szajdzinska-Pietek, E.; Pillars, T. S.; Schlick, S.; Plonka, A. *Macromolecules* **1998**, *31*, 4586.

(18) Martini, G.; Ristori, S.; Visca, M. In *Ionomers: Characterization, Theory, and Applications*; Schlick, S., Ed.; CRC Press: Boca Raton, FL, 1996; Chapter 10.

(19) Ottaviani, M. F.; Cossu, E.; Turro, N. J.; Tomalia, D. A. *J. Am. Chem. Soc.* **1995**, *117*, 4387 and references therein.

(20) *Pluronic and Tetronic Surfactants;* Technical Brochure; BASF Corp.: Parsipanny, NJ, 1989. Several formulas for L62 are given in the literature, depending on the molecular weight, all based on a EO content of 20% w/w: $EO_5PO_{30}EO_5$ in ref 1a (Figure 2) and ref 4a, corresponding to MW = 2188, and $EO_6PO_{34}EO_6$ in ref 1a (Table 1) and ref 6, corresponding to MW = 2500. We used the latter formula, for a more rounded MW value. We note that samples for phase diagram data and the samples reported in this study were prepared on a % w/w basis.

(21) In ref 17 we have reported on the variation of $a_N$ for the CAT*n* probes in water solutions with temperature: in the range 275−360 K the $a_N$ values decrease from 16.88 to 16.58 G (average values for CAT1, CAT8, and CAT16, within 0.05 G). The decrease of $a_N$ for CAT4, CAT8, and CAT16 with temperature is relatively small and can be related to the lowering of the dielectric constant, $\epsilon$, of the solvent: from $\epsilon \approx 85$ at 280 K to $\epsilon \approx 59$ at 360 K.[17]

(22) Schneider, J.; Freed, J. H. In *Biological Magnetic Resonance*; Berliner, L. J., Reuben, J., Eds.; Plenum Press: New York, 1989; Vol. 8, p 1.

(23) Kivelson, D. *J. Chem. Phys.* **1960**, *33*, 1094.

(24) Jolicoeur, C.; Friedman, H. L. J. *Solution Chem.* **1974**, *3*, 15.

(25) Nakagawa, T.; Jizomoto, H. *Colloid Polym. Sci.* **1979,** *257*, 502.

(26) Caragheorgheopol, A.; et al. To be submitted for publication.

(27) Lüsse, S.; Arnold, K. *Macromolecules* **1996**, *29*, 4251.

(28) Alexandridis, P.; Andersson, K. Submitted for publication in *J. Phys. Chem.*

(29) Vasilescu, M.; Caragheorgheopol, A.; Caldararu, H.; Bandula, R.; Lemmetyinen, H.; Joela, H. Submitted for publication in *J. Phys. Chem.*.

(30) Ristori, S.; Martini, G. *Langmuir* **1992**, *8*, 1941.

MA980982G